The reaction of fluorine atoms with silicon

Daniel L. Flamm, Vincent M. Donnelly, and John A. Mucha

Bell Laboratories, Murray Hill, New Jersey 07974
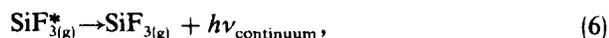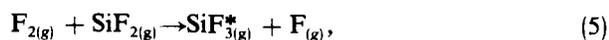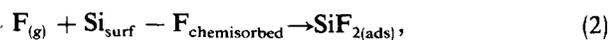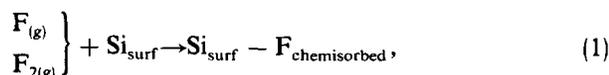
Fluorine atoms etch silicon with a rate, $R_{F(Si)} = 2.91 \pm 0.20 \times 10^{-12} T^{1/2} n_F e^{-0.108 \, eV/kT}$ Å/min, where n_F (cm^{-3}) is the atom concentration. This etching is accompanied by a chemiluminescent continuum in the gas phase which exhibits the same activation energy. These phenomena are described by the kinetics: (1) $F_{(g)} + Si_{surf} \rightarrow SiF_{2(g)}$, (2) $SiF_{2(g)} + F_{(g)} \rightarrow SiF_{3(g)}^*$, (3) $SiF_{2(g)} + F_{2(g)} \rightarrow SiF_{3(g)}^* + F_{(g)}$, (4) $SiF_{3(g)}^* \rightarrow SiF_{3(g)} + h\nu_{continuum}$ where formation of SiF_2 is the rate-limiting step. A detailed model of silicon gasification is presented which accounts for the low atomic fluorine reaction probability (0.00168 at room temperature) and formation of SiF_2 as a direct product. Previously reported etch rates of SiO_2 by atomic fluorine are high by a constant factor. The etch rate of SiO_2 is $R_{F(SiO_2)} = (6.14 \pm 0.49) \times 10^{-13} n_F T^{1/2} e^{-0.163/kT}$ Å/min and the ratio of Si to SiO_2 etching by F atoms is $(4.74 \pm 0.49)e^{-0.055/kT}$.

PACS numbers: 81.60. — j, 82.65.Nz

I. INTRODUCTION

A broad understanding of the rates and mechanisms by which free radicals react with various substrates is important for the development and selection of plasma-etching techniques. Although fluorine atoms are the principal gaseous reactant in many common etching processes, relatively little information is available on the reaction of these radicals with common semiconductor substrates. Recently, several investigators[1] have shown that an apparent continuum centered at 632 nm accompanies the etching of silicon by fluorine. Donnelly and Flamm [1a] studied the spectrum of the chemiluminescence and compared it with spectra from species in the discharge and afterglow regions of an SiF_4 discharge; they ascribed the chemiluminescence to the reactions:

$$\left. \begin{array}{c} F_{(g)} \\ F_{2(g)} \end{array} \right\} + Si_{surf} \rightarrow Si_{surf} - F_{chemisorbed}, \tag{1}$$

$$F_{(g)} + Si_{surf} - F_{chemisorbed} \rightarrow SiF_{2(ads)}, \tag{2}$$

$$SiF_{2(ads)} \rightarrow SiF_{2(g)}, \tag{3}$$

$$F_{(g)} + SiF_{2(g)} \rightarrow SiF_{3(g)}^*, \tag{4}$$

$$F_{2(g)} + SiF_{2(g)} \rightarrow SiF_{3(g)}^* + F_{(g)}, \tag{5}$$

$$SiF_{3(g)}^* \rightarrow SiF_{3(g)} + h\nu_{continuum}, \tag{6}$$

where spectral, kinetic and thermodynamic considerations were consistent with the view that the emitting radical is SiF_3. In other work the reaction probability for etching of silicon dioxide by F atoms and the etch ratio of Si to SiO_2 at room temperature was reported.[2]

In the present investigation, the etching of silicon by F atoms and intensity of the concomitant luminescence were measured as a function of temperature (223–403K) and F-atom concentration ($n_F = 1.6 \times 10^{15} - 7.7 \times 10^{15}$ cm^{-3}). The etching of SiO_2 at room temperature was also measured in order to determine simultaneously the ratio of Si and SiO_2 etch rates.

II. EXPERIMENTAL

The discharge-flow apparatus used for the etching of Si and SiO_2 by atomic fluorine is shown in Fig. 1. The discharge and flow arrangements have been described previously. [2a,1a] Single-crystal silicon samples (100) were bonded to the end of a 2.54-cm-o.d. aluminum rod (6061-T3) with epoxy and positioned in-line with the wall of a 2.54-cm-i.d. aluminum reaction cell.

The uncoated aluminum reaction cell had five ports through which the inlet tube, outlet tube, and silicon sub-
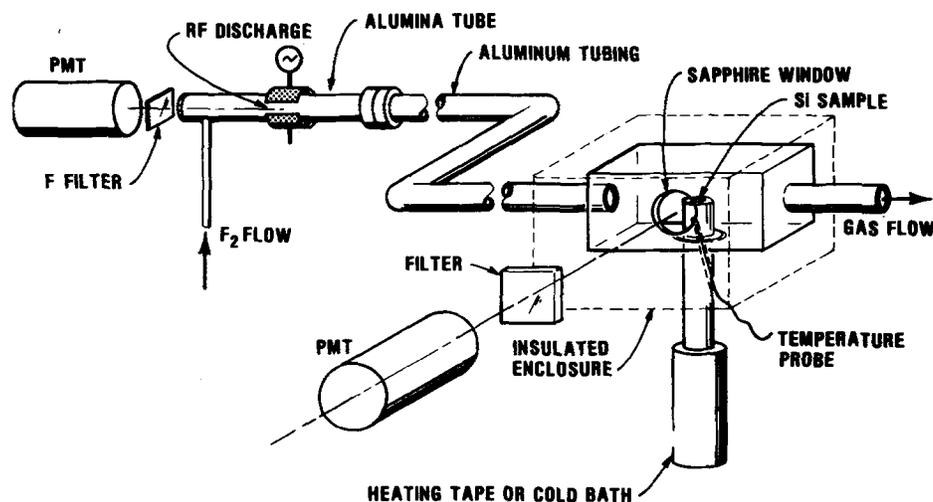

FIG. 1. Schematic of apparatus.

strate holder were sealed using Viton or Kalrez o-rings (Kalrez o-rings did not seal well at the lowest temperatures employed). The reaction cell was thermally insulated, while that part of the sample-holder rod (2.54-cm o.d. × 25.4-cm long) which extended out of the vacuum system was heated or cooled with electrical heating tape, a constant temperature bath, or a circulating refrigerant loop, depending on the desired temperature. A thermocouple was inserted into a thermowell just under the sample, and a second thermocouple was attached to the surface of the substrate holder immediately outside of the cell. The temperatures at these two stations were always in good agreement during the experiments, indicating that temperature gradients along the sample holder near and within the cell were negligible. The silicon samples were 0.05-cm thick and the epoxy had a thermal conductivity of 8×10^{-3} W/sec cm. A heat-transfer calculation including conduction, convection, radiation, and the heat of reaction, revealed that the sample surface is essentially isothermal in these experiments.

Fluorine atoms were generated by dissociation of F_2 (Air Products Technical Grade) in a 14-MHz-rf discharge 50-cm upstream of the reaction cell. Fluorine-atom concentrations were measured both upstream and downstream of the reaction cell by gas-phase titration with Cl_2.[2b,3] The average of these titrations (< 10% difference for all conditions) was used to interpret the data. Atom concentrations ranged from 1.0×10^{15} atoms/cm^3 at 3.8-W discharge power to 5.1×10^{15} atoms/cm^3 at 78 W with constant pressure (0.40 Torr) and F_2 flow (44 sccm), the conditions used in the etch-rate experiments. In emission experiments, the pressure was varied between 0.2 and 0.6 Torr (27–80 Pa) and the F_2 feed rate was between 18 and 70 sccm.

Chemiluminescence, originating in the gas phase above the Si (100) samples, was monitored through a 1-in-diam sapphire window which faced the sample in a direction perpendicular to the flow-tube axis and the sample surface normal. A cooled photomultiplier tube (RCA C31034) equipped with a 440-nm interference filter, 10 nm fullwidth at half maximum (FWHM) or Corning CS 2-61 long-pass red filter was used to monitor the emission.

Silicon etch rates were measured using samples having 10 000-Å-thick, 0.2-cm-wide parallel bars of steam-grown thermal oxide that covered 50% of the sample surface area. These bars were prepared by etching through a photoresist mask with 8:1 buffered HF, followed by acetone and methanol washes to remove the resist. In order to minimize or eliminate the presence of native oxide during the silicon etch studies, the bonded samples were immersed in buffered HF (BHF) for 20 sec, washed with deionized water, and blown dry with N_2 immediately before use. Samples were then sealed into the vacuum system and evacuated to several microns before starting the molecular fluorine flow. Several trials were also performed using samples that had been exposed to air for several weeks and not subsequently treated with HF before exposure to atomic fluorine (see below). After etching, the samples were removed from the rod by immersion in boiling dimethylformamide. The oxide mask was then dissolved in HF, and the etch depth was measured using a Sloan Technology Model 90050 Dektak stylus

thickness monitor.

Room-temperature SiO_2 etch rates and $Si:SiO_2$ etch ratios were determined using the same procedure, except that freshly patterned samples were always employed, and the photoresist-free pattern was not treated with BHF before use. Instead, long etch times were employed (> 30 min) to insure that the effect of any native oxide was negligible. Oxide thickness was measured before and after etching with a Nanospec AFT Model 174 microspectrophotometer; etching of the exposed silicon on these samples was measured as above.

III. RESULTS AND DISCUSSION
A. Silicon etch rates and chemiluminescence

Silicon etch depths varied from 6000 to 200 000 Å, depending on temperature, F-atom concentration, and etch time. The depth was uniform from "stripe" to "stripe" and along each stripe on all of the samples analyzed. This provides experimental evidence that reactant depletion and concentration-boundary-layer effects (diffusion control) can be ignored. While the depth etched was proportional to time, in general the exposed silicon adjacent to the oxide barmasks was etched slightly more than exposed silicon in the center of the stripes. This difference was $\lesssim 4000$ Å and did not vary with etch time. It appears that etching at the oxide-silicon boundary began somewhat earlier than etching at the center of the stripes. Perhaps a product of the BHF treatment tended to remain at this interface and minimized the initial regrowth of surface oxide.

Chemiluminescence was continuously monitored during all of the runs on masked samples. In some of the early experiments, before special attention was given to surface cleaning, we noted a delay in chemiluminescense and etching. For instance, in one set of four runs ($n_F = 4.0 \times 10^{15}$ cm^{-3}, $T = 296$ K) the initial luminescence was relatively weak; but after a period of time there was a rapid and dramatic (10–30 fold) increase in chemiluminescent intensity. Three samples, which had been exposed to air for several weeks and were not treated with buffered HF before etching, showed a latency of ≈ 8 min. When the etching time for these runs was plotted as a function of etch depth and extrapolated to zero depth, a positive intercept was obtained (i.e., an induction period for etching). This induction period was in excellent agreement with the corresponding chemiluminescent latency. The fourth air–exposed substrate was dipped in buffered HF solution for 20 sec immediately before etching. The emission-versus-time trace was similar to the above runs, except that the latency was reduced from 8 to ≈ 2 min. Thus, it may be concluded that the delay in luminescence was associated with the removal of a surface layer (native oxide or more likely some other contamination).

In subsequent work, uncertainties in the onset of etching were overcome by using freshly prepared samples, *always* treating the samples with HF solution prior to etching (as described above), and etching for times much longer than the latencies noted in early experiments. Extrapolation of etch depth versus time to $t = 0$ (discharge turned on) showed little or no induction period in these runs. The latency in emission also was not present in later experiments; instead, a

very intense transient emission was observed at $t = 0$ which decayed in ~ 1 min.

After the initial step change in luminescent intensity, a very gradual increase in luminosity ($\sim 2\%$/min for the first 20 min) was always observed. At room temperature and $n_F = 4 \times 10^{15}$ cm^{-3}, fresh, unpatterned samples reached a constant "saturation luminosity" after ~ 40 min. As a sample is etched the surface roughness increases, and the slow increase in chemiluminescence is probably associated with a change in surface texture.

B. Emission and silicon etching versus temperature

The saturated intensity (see Sec. III A) was measured as a function of temperature. Figure 2 shows a typical data set taken at constant pressure and mole fraction of F atoms (constant discharge power), which has been corrected for the effect of temperature on gas-phase F-atom density $[n_F(T) = n_{F(296)} \times (296/T)]$. The intensity is well described by an Arrhenius expression:

$$I = I_0(273/T)^{1/2}e^{-E_i/kT}, \tag{7}$$

where the factor $(273/T)^{1/2}$ corrects for the temperature dependences of atom concentration and atom flux to the surface; k is the Boltzman constant. The slope of these data corresponds to an activation energy E_i of 0.101 eV (2.33 kcal/mole). Table I presents E_i's independently determined from regression of four different experimental conditions. The weighted average activation energy for these five experiments is 0.116 ± 0.012 eV (2.68 ± 0.28 kcal/mole). The maximum deviation of any one run from the mean is 15%, indicating little if any dependence on pressure, flow, atom concentration, or spectral region over a fairly wide parameter space.

Figure 2 also shows the temperature dependence of etch rates similarly corrected for the effect of temperature on atom density. These etch rates are described by the regression equation

$$R_{(Si)} = 2.91 \pm 0.20 \times 10^{-12} n_F T^{1/2}e^{-E_{etch}/kT}. \tag{8}$$

Least-squares analysis yields an activation energy $E_{etch} = 0.108 \pm 0.005$ eV ($2.49 : 0.12$ kcal/mole). Within experimental error the etch rate and chemiluminescent intensity have the same activation energy.

The activation energy derived from the etch-rate data is associated with the slowest step in the etching reaction. In emission experiments, the intensity at any given temperature is a measure of the yield of SiF$_2$ relative to all fluorosilicon desorption products. Regardless of which step is rate-limit-
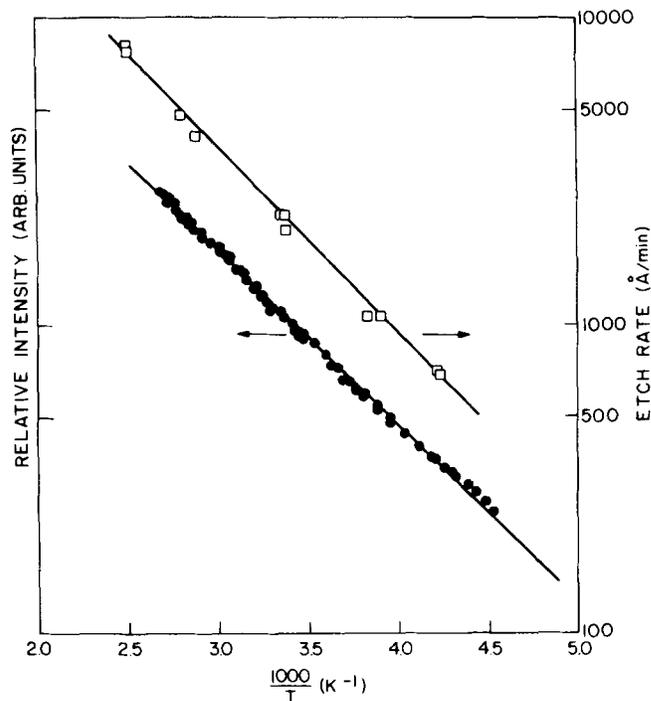

FIG. 2. Silicon etch rate and chemiluminescence vs 1000/T for $n_F = 2.9 \times 10^{15}$. Intensity data group corresponds to Run 1, Table I.

ing, the activation energies in the two sets of experiments can agree in only two circumstances: (1) the fraction of SiF$_2$ relative to all SiF$_x$ desorption products is temperature independent, or (2) the chemiluminescence and etching are associated with the same rate-limiting process—implying that SiF$_2$ is the primary etch product. These two cases are treated in detail below (Sec. III.E.).

The probability $\epsilon_{F(Si)}$ of an impinging fluorine atom undergoing reaction with silicon may be defined as

$$\epsilon_{F(Si)} = 4N_a\rho_{Si}R_{Si}/M_{Si}\left[\tfrac{1}{4}(n_F v)\right], \tag{9}$$

where N_a is Avogrado's number, ρ_{Si} is the density of silicon, M_{Si} is the atomic weight of silicon (28.09), n_F is the gas-phase number density of atomic fluorine, v is the mean thermal velocity [equal to $(8kT/\pi M_F)^{1/2}$] and $\tfrac{1}{4}n_F v$ is the flux of atoms to the surface. In deriving Eq.(9), the factor of 4 in the numerator arises from the assumption that SiF$_2$ is a minor desorption product and that the major reaction product formed on the surface from F atoms is SiF$_4$ ($\epsilon_{F(Si)}$ would be half as large if SiF$_2$ were the major product). This assumption is dictated by the arguments presented in Sec. III E (but

TABLE I. Chemiluminescence activation energies. Weighted mean: $E_i = 0.116 \pm 0.012$ eV.

Run	E_i (eV)	Pressure (Torr)	Flow (sccm)	Power (W)	Temperature Range (K)	Filter Type	No. of Points
1	0.102	0.56	70	18	221–373	CS-2-61	72
2	0.120	0.58	70	40	309–373	CS-2-61	16
3	0.135	0.54	18	40	243–393	440 nm	40
4	0.123	0.54	18	40	297–379	440 nm	16
5	0.121	0.27	18	38	233–373	440 nm	62

see Ref. 16). $\epsilon_{F(Si)}$ is given by the regression equation

$$\epsilon_{F(Si)} = 0.1162 \pm 0.0080e^{-E_{etch}/kT}, \qquad (10)$$

where $E_{etch} = 0.108 \pm 0.005$ and $\epsilon_{F(Si)}$ ranges from 0.00168 at room temperature (23 C) to 0.0040 at 100 C.

C. Silicon etching and emission versus F-atom concentration

In the above discussion, it has been implicitly assumed that the etching of silicon is proportional to F-atom concentration. Figure 3 does indeed show that the etch rate changes linearly with F-atom concentration as it is varied by changing the discharge power. Furthermore, the intercept is not significantly different from zero, in accord with the independent experimental finding[4] that the rate of silicon etching by *molecular* fluorine (~ 3 Å/min at 300 K) is negligible compared with present etch rates (1000–4000 Å/min).

Unlike etching, the intensity of chemiluminescence does not increase linearly with F-atom concentration (Fig. 3). Equations (2)–(5) suggest that the luminescent intensity should be given by[5]

$$\frac{I}{n_F} = \left(\frac{\Phi_4 k_4 n_F}{\Phi_5 k_5 n_{F_2}} + 1 \right) \bigg/ \left(\frac{k_4 n_F}{k_5 n_{F_2}} + 1 \right), \qquad (11)$$

where the first term in the numerator arises from the reaction of SiF$_2$ $[n_{SiF_2} \propto k_2 n_F \ (k_4 n_F + k_5 n_{F_2})]$ with atomic fluorine in Eq. (4), and the second term corresponds to reaction with molecular fluorine, Eq. (5). Φ_4 and Φ_5 are the fractional yields of SiF$_3^*$, relative to all products arising from the reaction of SiF$_2$ with F and F$_2$, respectively. A plot of I/n_F against n_F/n_{F_2} along with the least-squares fit to Eq. (11) are shown in Fig. 4; the data are in excellent agreement with this model. From the fit, $k_4/k_5 = 8.5$, so that reaction (4) is from 1.5–7.5 times faster than reaction (5) over the range of our
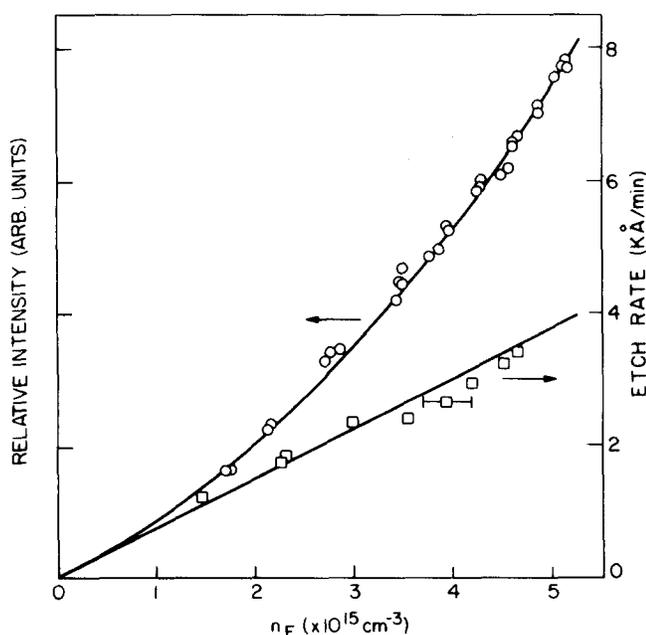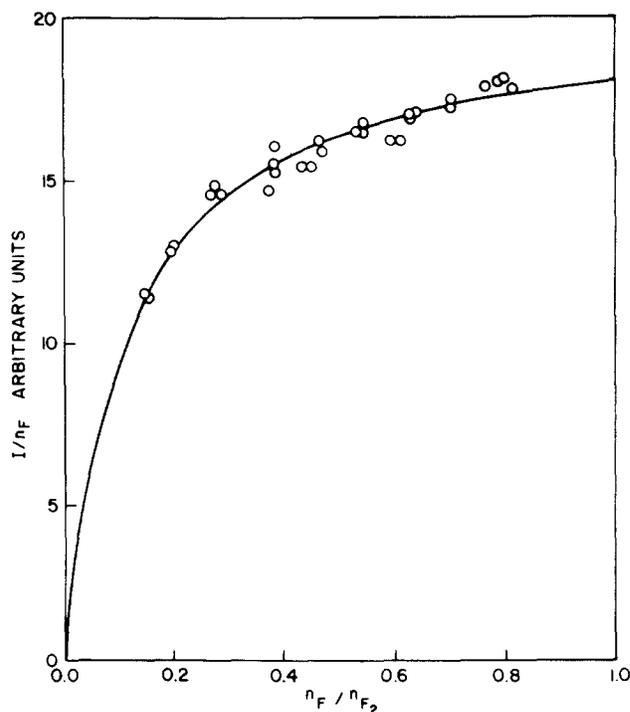

FIG. 4. $I/n_F n_{F_2}$ vs n_F/n_{F_2} at room temperature (296 K). These intensity data are also shown in Fig. 3.

data. The least-squares analysis also yields $\Phi_4/\Phi_5 \approx 100$. The agreement is sensitive to the value of k_4/k_5, but does not depend strongly on Φ_4/Φ_5; hence it is concluded $20 \lesssim \Phi_4/\Phi_5 \lesssim 120$.

At the present pressure, the reaction of SiF$_2$ with F could conceivably proceed by a termolecular mechanism, but a choice between bi- and termolecular models on the basis of the present data would be arbitrary. However, it is significant that the reaction of SiF$_2$ with *both* atomic *and* molecular fluorine must be included in either model to explain the relationship between luminescence and F-atom concentration. Our observations of a chemiluminescence during the etching of Si by molecular fluorine [4c] provide further evidence for reaction (5). Smolinsky and Flamm[6] also presented indirect evidence for this process. Additional experiments to confirm steps (4)–(6) are now in preparation. This will involve adding F and F$_2$ to a flow of SiF$_2$ formed in the high-temperature reaction of SiF$_4$ with solid Si.[7]

D. SiO$_2$ etch rates and Si:SiO$_2$ etch ratio

The etch rates of SiO$_2$ and Si were simultaneously measured as a function of F-atom concentration at room temperature. Both rates were proportional to n_F with an intercept at the origin (95% confidence level). The silicon etch-rate data from these experiments are included in Fig. 3.

In the course of this work, we discovered a systematic inconsistency between our data and previously reported SiO$_2$ etch rates. [2a] A number of significant improvements (such as the installation of linear mass flowmeters and a pressure controller) have been made in the present apparatus since that early study, and it was possible to reexamine the

FIG. 3. Etch rate and chemiluminescence vs n_F at room temperature (296 K).

previous raw etch-rate data and flow calibrations. A systematic error in Cl_2 flow calibration was found to influence the previous results. When this is taken into account, the correct atom concentration applicable to the study of Flamm *et al.* [2a] is found to be $n_F \sim 9.3 \times 10^{15}$. It follows that the previously reported rates were high by a constant factor of ~ 1.5.

Using corrected raw data from Ref. 2a together with the present room-temperature SiO_2 etch rates, the etch rate of SiO_2 by F atoms becomes

$$R_{F(SiO_2)} = 6.14 \pm 0.49 \times 10^{-13} n_F T^{1/2} e^{-0.163/kT} \text{ Å/min}, \quad (12)$$

and the reaction probability for SiO_2 is

$$\epsilon_{F(SiO_2)} = 0.0112 \pm 0.0009 e^{-0.163/kT}, \quad (13)$$

where it is *assumed* that the final reaction product formed on the surface of SiO_2 by F atoms is SiF_4.

Combining Eqs. (8) and (12), the ratio of the Si etch rate to that of SiO_2 is

$$R_{F(Si)}/R_{F(SiO_2)} = 4.74 \pm 0.49 \, e^{0.055/kT}, \quad (14)$$

which ranges from 41.0 at room temperature to 26.2 at 100 C. The room-temperature etch ratio (42:1), which Flamm [2b] calculated from preliminary Si etch data (based on the previous (high) atomic-fluorine calibrations) is in good agreement with the present result (41 ± 4).

E. Reaction of a silicon surface with atomic fluorine: mechanism

Recent work[8] provides evidence that fluorine atoms form a stable chemisorbed layer on the surface of single crystal silicon. Consider a $\langle 100 \rangle$ silicon surface. Since Si atoms have two free bonding sites per atom, it can be anticipated that fluorine atoms will react to form a periodic array of SiF_2 groups on the surface. Each of these groups is, in turn, bound to two Si atoms in the bulk crystal:

$$(15)$$
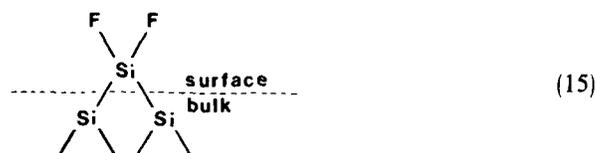
Electron spectroscopy for chemical analysis (ESCA) supports this detailed picture.[8] After silicon is etched by XeF_2, fluorine remains bound to the surface with bonds that exhibit a chemical shift similar to that of SiF_2 molecules. A study of infrared emission from a silicon surface during XeF_2 etching also suggests a fluorinated surface.[8,9] The radiation is polarized and wavelengths are consistent with known Si-F-bond absorptions.

At steady state during etching, some incident F atoms may be expected to physisorb as a secondary layer on the SiF_2-like surface. Since $\epsilon_{F(Si)}$ is small, it follows that most fluorine in this secondary layer simply desorbs. Our experiments show that the Si etch rate is directly proportional to the impingement rate of F atoms from the gas phase (at least within the present range of $n_F \lesssim 6 \times 10^{15} \text{cm}^{-3}$). This fact, together with the low value of $\epsilon_{F(Si)}$, suggest that surface coverage (θ_F) by the physisorbed fluorine layer is sparse and that recombination of physisorbed atoms is likely to be slow compared with desorption. The same conclusion can be reached by a statistical thermodynamic calculation of coverage[10] giving $\theta_F \lesssim 10^{-4}$ for a Langmuir isotherm with parameters corresponding to physical adsorption ($\lesssim 5$ Kcal heat of adsorption and an oscillator frequency $\nu \sim 10^{12} \text{ sec}^{-1}$).
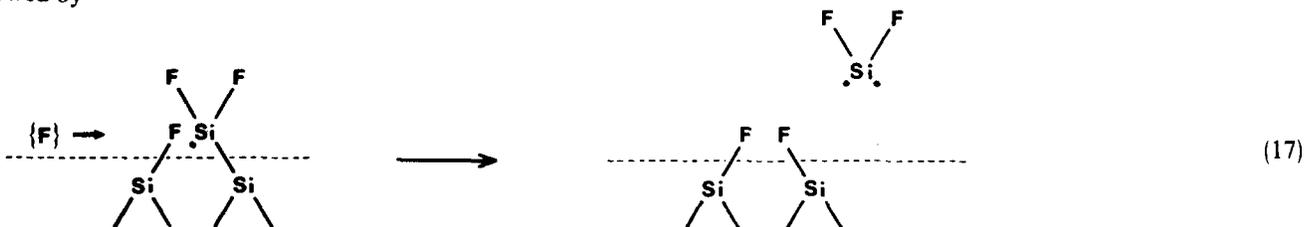
Chemisorbed SiF_2 groups may be ultimately gasified by the reaction of impinging atoms with an Si-Si bond:

$$(16a)$$

or by

$$(16b)$$

followed by

$$(17)$$
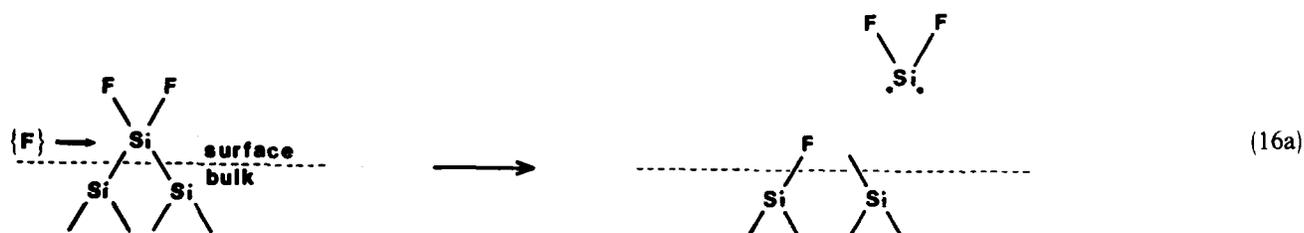
Explore Litigation Insights

Docket Alarm provides insights to develop a more informed litigation strategy and the peace of mind of knowing you're on top of things.

Real-Time Litigation Alerts

Keep your litigation team up-to-date with **real-time alerts** and advanced team management tools built for the enterprise, all while greatly reducing PACER spend.

Our comprehensive service means we can handle Federal, State, and Administrative courts across the country.

Advanced Docket Research

With over 230 million records, Docket Alarm's cloud-native docket research platform finds what other services can't. Coverage includes Federal, State, plus PTAB, TTAB, ITC and NLRB decisions, all in one place.

Identify arguments that have been successful in the past with full text, pinpoint searching. Link to case law cited within any court document via Fastcase.

Analytics At Your Fingertips

Learn what happened the last time a particular judge, opposing counsel or company faced cases similar to yours.

Advanced out-of-the-box PTAB and TTAB analytics are always at your fingertips.

API

Docket Alarm offers a powerful API (application programming interface) to developers that want to integrate case filings into their apps.

LAW FIRMS

Build custom dashboards for your attorneys and clients with live data direct from the court.

Automate many repetitive legal tasks like conflict checks, document management, and marketing.

FINANCIAL INSTITUTIONS

Litigation and bankruptcy checks for companies and debtors.

E-DISCOVERY AND LEGAL VENDORS

Sync your system to PACER to automate legal marketing.

fastcase®
Smarter legal research.